Supplementary Material (ESI) for Chemical Communications
This journal is (c) The Royal Society of Chemistry 2011

SUPPORTING INFORMATION

Aerosol-Spraying Preparation of Mesoporous Hollow Spherical $BiFeO_3$ Visible Photocatalyst with Enhanced Activity and Durability

Yuning Huo, Miao Miao, Yi Zhang, Jian Zhu and Hexing Li*

The Education Ministry Key Lab of Resource Chemistry, Shanghai Normal University, Shanghai 200234, P.R. China.

Summary: 16 Pages; 11 Figures and 2 Schemes

Experimental details

Catalyst preparation

The $BiFeO_3$ was synthesized in an aerosol-spraying reactor (Fig. S1). In a typical run of synthesis, 1.1 g $Bi(NO_3)_3 \cdot 5H_2O$ was dissolved in 48 mL ethanol containing desired glycerol. Then, 0.81 g $Fe(NO_3)_3 \cdot 9H_2O$ was added and stirred until the clear solution was obtained. Subsequently, the solution was atomized into aerosol droplets and then passed through a quartz glass tube at 800 ^oC with N_2 carrier gas (4.0 L/min). The solid particles collected on a filter were then calcined for 4 h at desired temperature to remove organic residues and promote crystal growth. The as-prepared samples were denoted as BFO-X-Y, where X and Y represent the glycerol amount (mL) in the initial aerogel solution and calcination temperature (^oC), respectively. The samples before calcination were denoted as BFO-X. BFO-X-Y(G) represents the $BiFeO_3$ particles obtained by crushing the BFO-X-Y hollow spheres. For comparison, the $BiFeO_3$ in solid particles, denoted as BFO-SSR, was also prepared by solid-state reaction at 800 ^oC for 5 h following the procedures reported previously.[7]

Characterizations

The structure was examined by Fourier transform infrared spectrometer (FTIR, NEXUS 470, samples pelletized with KBr, 32 scanning times) and X-ray diffraction (XRD, Rigacu D/Max-2000, monochromatic CuKa radiation, graphite curve monochromator, 0.02°(2 θ) Scan step, 4°/min scan rate, 40 kV voltage, 30 mA current). Crystallite sizes were determined based on the Scherrer equation ($D = K\lambda/\beta cos\theta$). Surface morphology was observed by transmission electronic microscopy (TEM, JEM-2010). X-ray photoelectron spectroscopy (XPS, Versa Probe PHI 5000, Al Kα excitation sourse, 10^{-9} torr pressure in analysis chamber, 14.0 kV voltage) was employed to determine surface electronic states. The shift of the binding energy due to relative surface charging was corrected using the C_{1S} level at 284.8 eV as an

internal standard. Samples were pelletized into 5×5 mm sheet before measurement. N_2 adsorption-desorption isotherms were measured on a Quantachrome NOVA 4000e at 77 K. The Brunauer-Emmett-Teller (BET) method was used to calculate the specific surface area (S_{BET}) and the Barrett-Joyner-Halenda (BJH) model was used to calculate pore volume (V_P) and pore diameter (D_P). The thermal stability was investigated by a thermogravimetric analyzer (DTG-60H, 10 ^{o}C/min heating rate, 50 mL/min flow rate, referenced Al_2O_3 sample). The light absorption ability was analyzed by UV-vis diffuse reflectance spectra (DRS, MC-2530).

Activity test

The rhodamine B (RhB) photodegradation was carried out at 303 K in a self-designed quartz reactor containing 50 mL of 1.0×10^{-5} M RhB and 0.10 g catalyst. The mixture was stirred vigorously at the speed of 800 rpm to eliminate diffusion effect on the reaction kinetics. After reaching adsorption equilibrium, the photocatalytic reaction was initiated by irradiating with one 500 W Xe lamp (CHF-XM500, light intensity = 600 mW/cm^2) located at 18 cm above the solution surface. To make sure that the photocatalytic reaction was really driven by visible lights, the lights with wavelength less than 420 nm were cut off by a glass filter (JB-420). Each run of reactions was lasted for 6 h and the unreacted RhB was analyzed by a UV spectrophotometer (UV 7504/PC) at their characteristic wavelength of 553 nm to determine the degradation yield. Preliminary experiments demonstrated that only less than 8% RhB was decomposed after reaction for 6 h in the absence of either the photocatalyst or light irradiation, and thus could be neglected in comparison with degradation yield resulting from photocatalysis. The reproducibility of the results was checked by repeating each reaction at least three times and was found to be within acceptable limits (± 5 %).

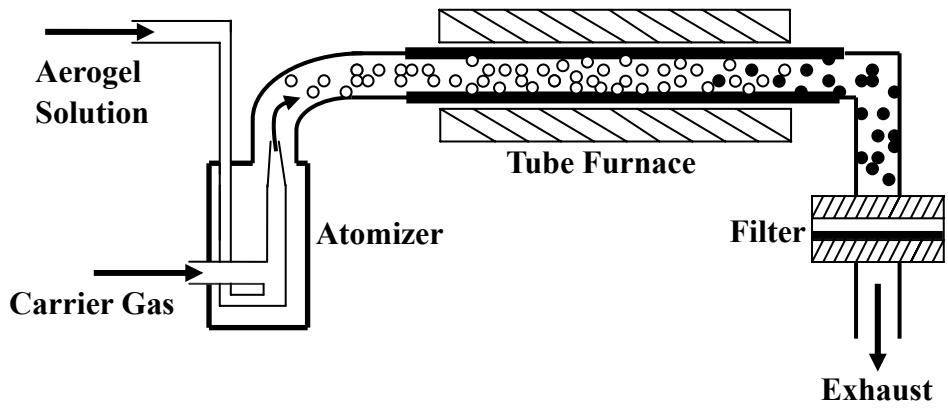

Fig. S1 Schematic diagram of aerosol-spraying reactor.

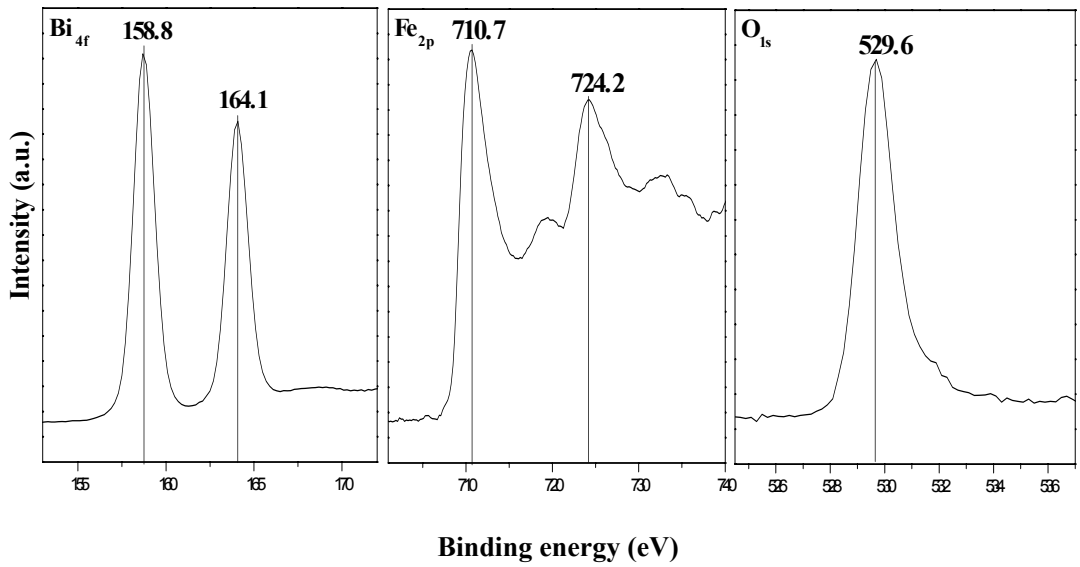

Fig. S2 XPS spectra of BTO-2-500 sample.

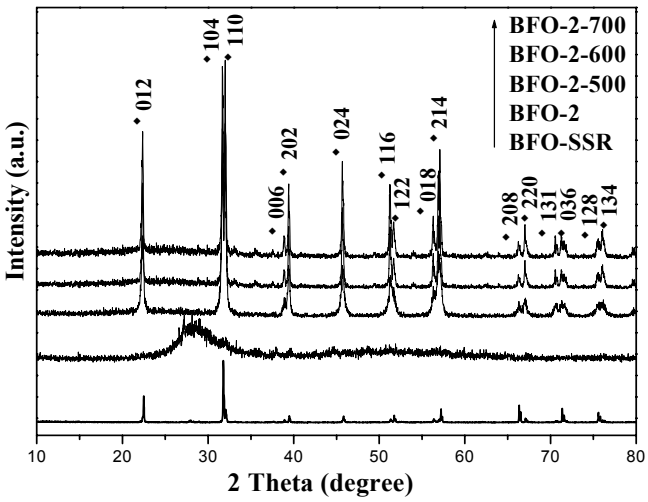

Fig. S3 XRD patterns of different BFO samples.

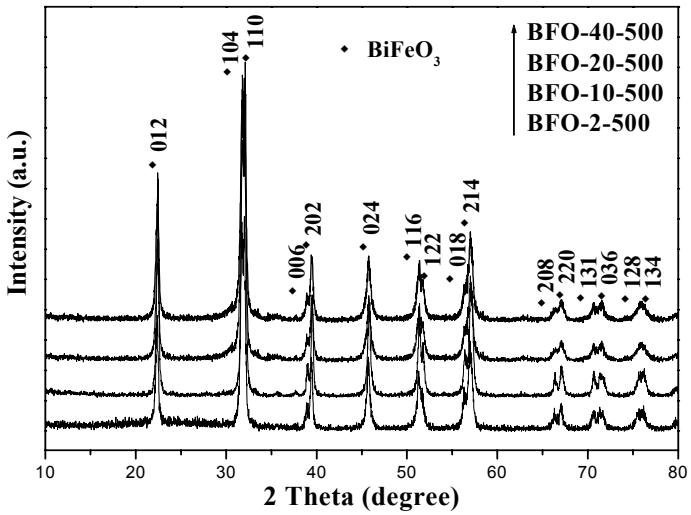

Fig. S4 XRD patterns of BFO-X-500 samples calcined at 500 ^{o}C.

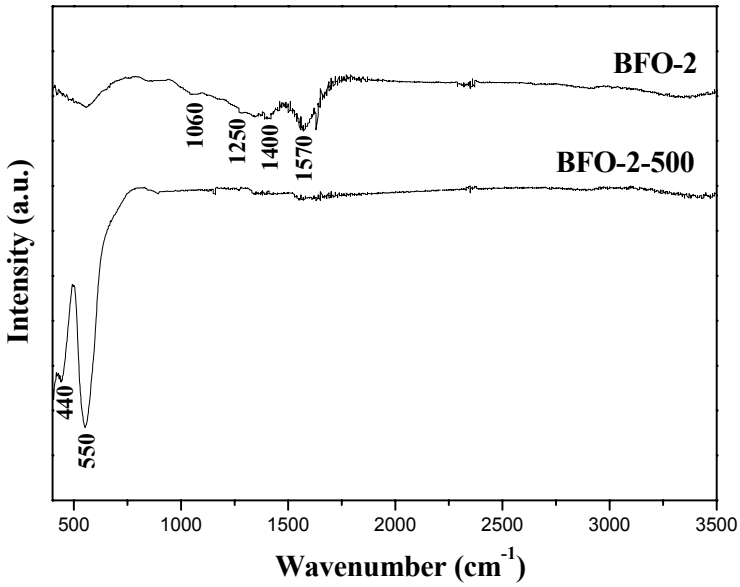

Fig. S5 FTIR spectra of BFO-2-500 calcined at 500 ^{o}C and BFO-2 before calcination.

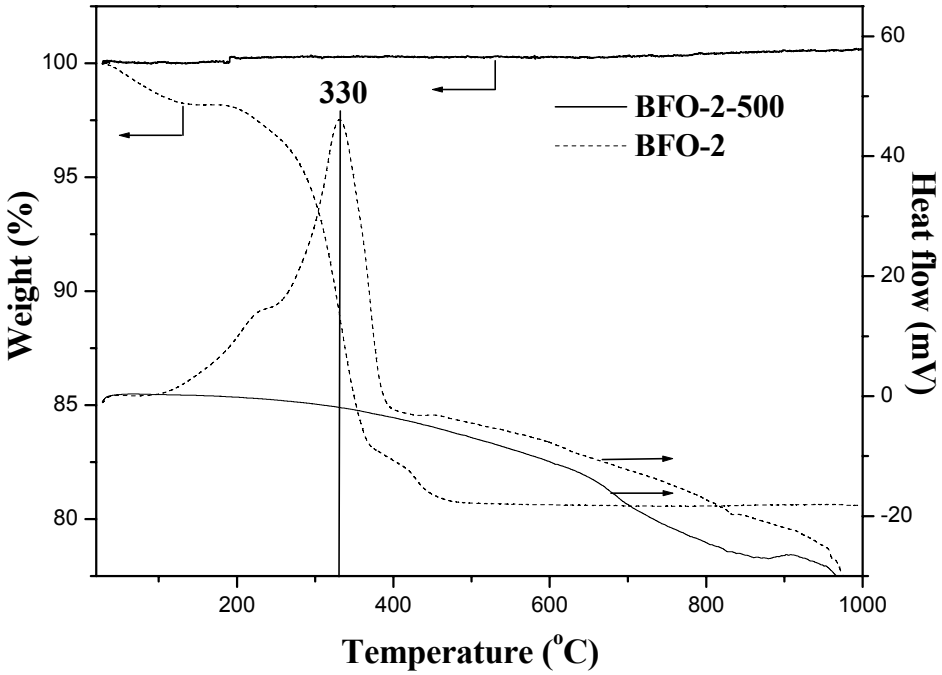

Fig. S6 TG/DTA curves of BFO-2-500 calcined at 500 °C and BFO-2 before calcination.

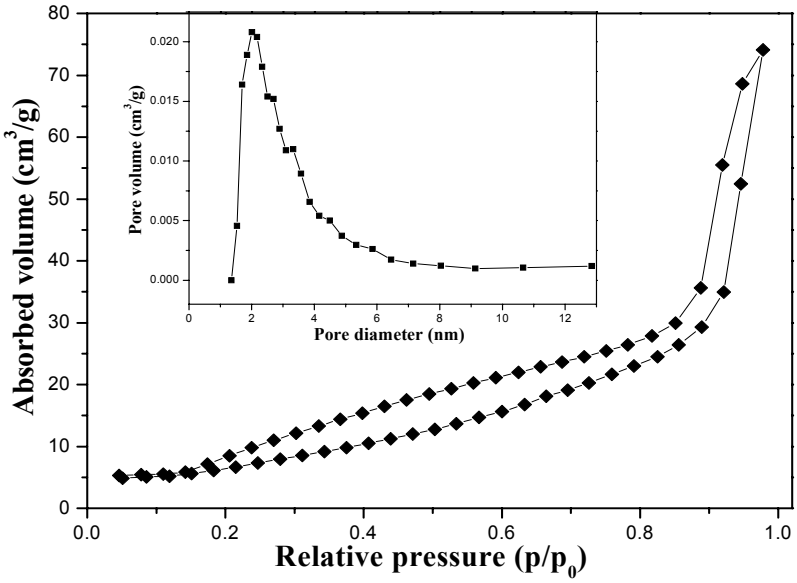

Fig. S7 Nitrogen adsorption-desorption isotherm and pore size distribution (inset) of BFO-2-500.

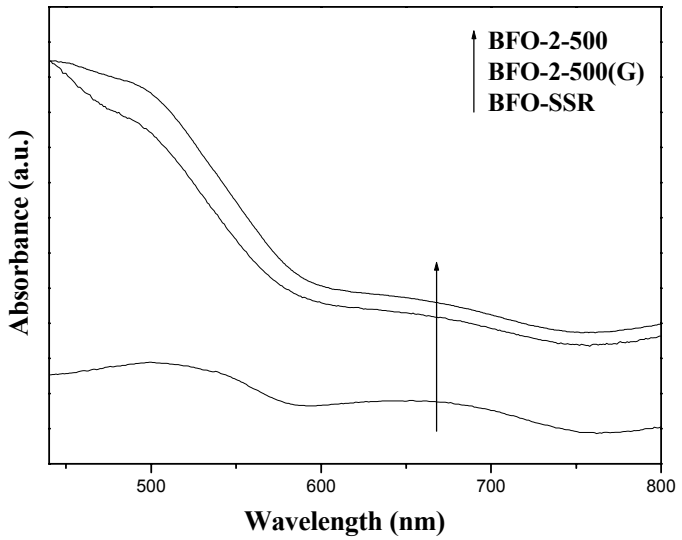

Fig. S8 UV-Vis DRS spectra of BFO-2-500, BFO-2-500(G) and BFO-SSR.

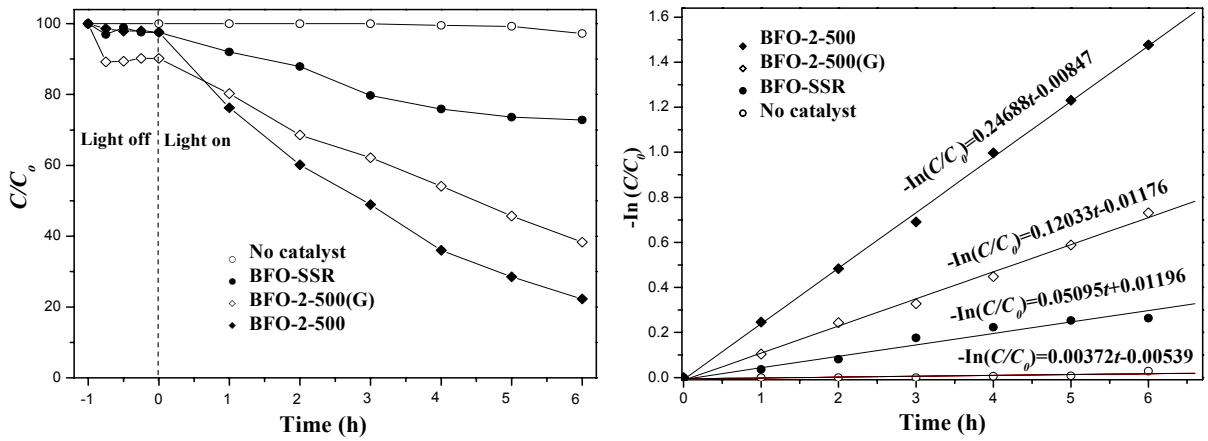

Fig. S9 Reaction process (left) and the kinetic relationship (right) for the photocatalytic degradation of RhB. C_0 and C refer to the initial RhB concentration and the RhB concentration determined at different reaction time.

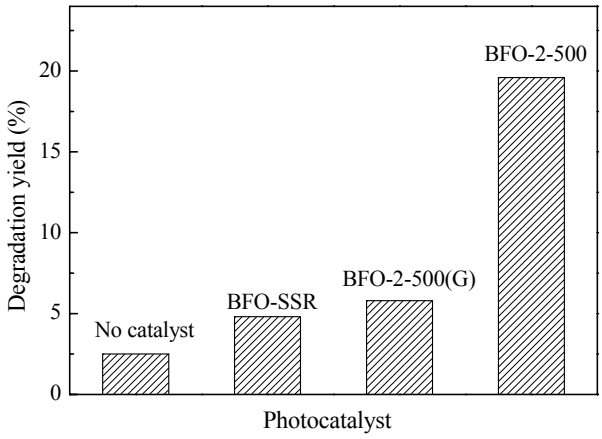

Fig. S10 Photodegradation of 4-chlorophenol (4-CP) over different catalysts under visible irradiation. Reaction conditions: 50 mg catalyst, 30 mL aqueous solution of 1.0×10^{-4} M 4-CP, reaction temperature = 30°C, reaction time = 4 h, one 500 W Xe lamp (light intensity = 600 mW/cm^2, wavelength > 420 nm).

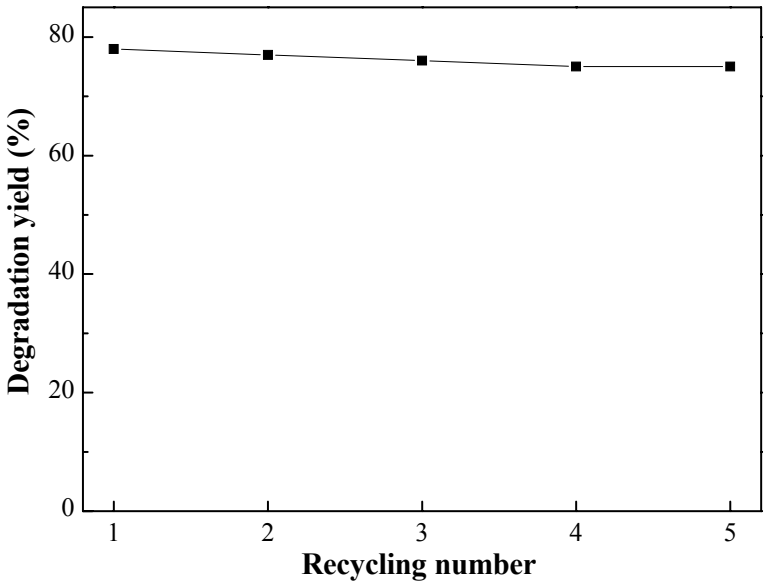

Fig. S11 Recycling test of the BFO-2-500 catalyst. Reaction conditions: 0.10 g catalyst, 50 mL solution of 1.0×10^{-5} M RhB, reaction temperature = 30°C, one 500 W Xe lamp (light intensity = 600 mW/cm^2, wavelength > 420 nm). Each run of photocatalytic reactions lasted for 6 h.

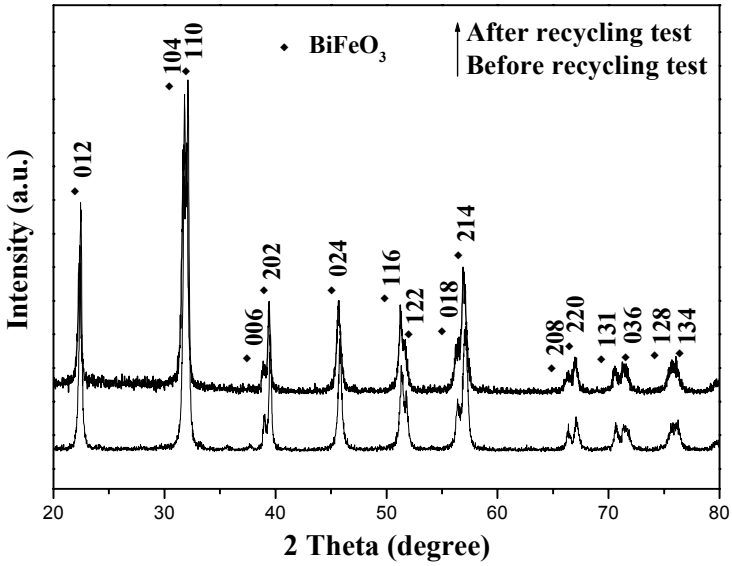

Fig. S12 XRD patterns of the fresh BFO-2-500 and the BFO-2-500 after being used repetitively for 5 times.

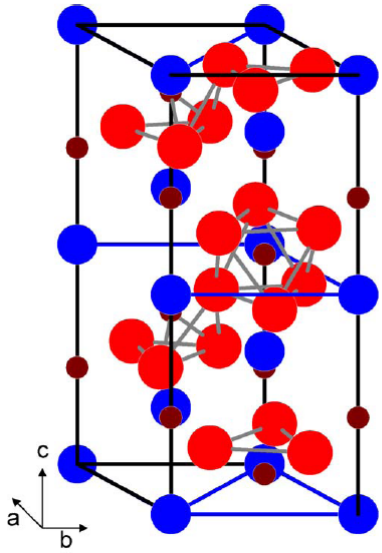

Scheme S1 Structure of *R3c* rhombohedral cell in perovskite-type $BiFeO_3$. (● = Bi, ● = O, ● = Fe)

$BiFeO_3$ hollow sphere with thin shell **$BiFeO_3$ hollow sphere with thick shell**

Scheme S2 Effect of the shell thickness on the light absorbance model.